

# Pregnancy in the Brown Norway Rat: A Model for Investigating the Genetics of Placentation<sup>1</sup>

Toshihiro Konno, Lea A. Rempel, Juan A. Arroyo,<sup>3</sup> and Michael J. Soares<sup>2</sup>

*Institute of Maternal-Fetal Biology and the Division of Cancer and Developmental Biology, Department of Pathology and Laboratory Medicine and Obstetrics and Gynecology, University of Kansas Medical Center, Kansas City, Kansas 66160*

## ABSTRACT

The placenta facilitates the exchange of nutrients and wastes in an effort to promote fetal development. Disruptions in the establishment of the placenta and its interactions with the maternal uterus are potential causes of pregnancy failure. In this study we investigated the pregnancy phenotype of two inbred rat strains: the Dahl Salt Sensitive (DSS) strain and the Brown Norway (BN) strain. The DSS strain is reported to have large litters, whereas the BN strain has small litters. Pregnant female rats of each strain were killed on various days of gestation. At the time of killing, the number of viable versus dead and/or resorbing conceptuses was determined. Placental tissues from viable conceptuses were collected and processed for biochemical and histologic analyses. The number of viable conceptuses at Days 8.5 and 18.5 of gestation was significantly greater in DSS versus BN rats. Additionally, the number of resorbing and/or dying conceptuses was significantly greater in the BN strain than in the DSS strain. Maternal responses to pregnancy and elements of placental and fetal development in DSS and BN rats differed. Immunohistologic analysis of placentation and gene expression profiles revealed that trophoblast cell invasion into the uterine mesometrial compartment was significantly less in the BN strain versus the DSS strain. In contrast, the uterine natural killer cell population was reciprocally expanded in the BN strain. The impairment in trophoblast cell invasion in BN rats was associated with a smaller junctional zone compartment of the chorioallantoic placenta. Collectively, the data indicate that BN rats exhibit a unique form of placentation and may represent an excellent model for investigating the genetics of placental development.

*natural killer cells, placenta, pregnancy, pregnancy invasive trophoblast, prolactinlike proteins, trophoblast*

## INTRODUCTION

Pregnancy is a complicated biologic process that requires a dynamic interaction between embryonic and maternal tissues. Fertilization activates cell division of the embryo. As the embryo increases in size, some of its cellular constituents become exposed to different environments, marking an early

trigger to differentiation of trophoblast and inner cell mass lineages [1]. Trophoblastic lineages develop into parts of the placenta, while the inner cell mass lineages form embryonic and some extraembryonic structures. Simultaneously, the maternal endocrine system signals critical changes in the mother's tissues, especially the uterus [2]. A striking interdependence ensues between mother and embryo. Virtually every tissue and physiologic process within the mother is impacted by pregnancy [3–5]. Maternal metabolic, vascular, and immune systems are modified to enrich nutrient flow to the embryo/fetus and to promote embryonic/fetal survival. Ineffective adaptive mechanisms to pregnancy culminate in disease and negative outcomes for the embryo/fetus. Experiences during the prenatal period have lasting effects, influencing postnatal and adult disease processes [6–8]. Molecular mechanisms and signaling events involved in the establishment and maintenance of pregnancy have not been adequately determined.

The objective of this research project was to identify model systems for investigating the genetics of pregnancy and placentation. We have selected the rat for our analysis because of its demonstrated utility in studying complex biologic functions [9]. In this report, we provide insights into the placentation-related phenotypes of two inbred rat strains (Dahl Salt Sensitive [DSS] and Brown Norway [BN]). The DSS and BN inbred rat strains were selected for the analysis because they possess distinctive reproductive characteristics. DSS rats breed well and have large litters, whereas BN rats breed poorly and have small litters [10, 11]. We report that the BN rat possesses a distinct placentation phenotype, including a profound impairment in intrauterine trophoblast cell invasion, a growth-restricted junctional zone compartment of the chorioallantoic placenta, and compensatory increases in uterine natural killer (NK) cells.

## MATERIALS AND METHODS

### *Animals and Tissue Preparation*

BN and DSS inbred rats were obtained from Charles River Laboratories (Wilmington, MA). ACI inbred and Holtzman Sprague-Dawley outbred rats were purchased from Harlan Sprague-Dawley (Indianapolis, IN). Animals were housed in an environmentally controlled facility, with lights on from 0600–2000 h, and were allowed free access to food and water. DSS and BN inbred rats were maintained on low-salt diets obtained from Harlan Teklad (3075S; Madison, WI) or Purina (5010; Richmond, IN). ACI and Holtzman Sprague-Dawley rats were provided a standard rodent laboratory diet (8604; Purina). Under these dietary conditions the DSS strain does not exhibit significant kidney or blood pressure pathologies. Additionally, pregnancy and placentation is similar in BN rats fed all of the above diets. Virgin female rats 8–10 wk of age for each strain were cohoused with adult males (>3 mo of age) of the same strain. Mating was assessed by daily inspection of vaginal lavages. The presence of sperm in the vaginal lavage was considered as Day 0.5 of pregnancy. Some pregnant DSS and BN female rats were weighed daily and killed on Day 18.5 of gestation, whereas others were not handled until killing on Gestation Days 8.5, 11.5, 13.5, 15.5, 18.5, or 21.5. At the time of killing, placental and fetal tissues were collected and weighed. The number of viable

<sup>1</sup>Supported by grants from the National Institutes of Health (HD20676, HD39878, HD48861, and HD49503) and the Hall Family Foundation.

<sup>2</sup>Correspondence: Michael J. Soares, Institute of Maternal-Fetal Biology, Department of Pathology and Laboratory of Medicine, University of Kansas Medical Center, 3901 Rainbow Blvd., Kansas City, KS 66160. FAX: 913 588 8287; e-mail: msoares@kumc.edu

<sup>3</sup>Current address: Department of Obstetrics and Gynecology, University of Colorado Health Sciences Center, Aurora, CO 80045.

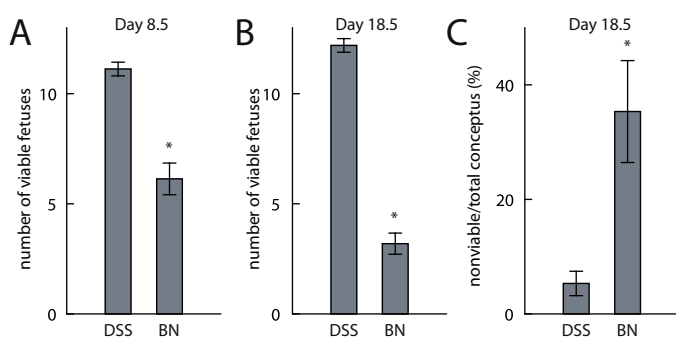


FIG. 1. Reproductive efficiency of DSS and BN rat strains. **A)** Viable conceptuses in DSS and BN strains on Day 8.5 of pregnancy. The number of viable conceptuses for the BN strain was significantly lower than that observed for the DSS strain on Day 8.5 of gestation,  $*P < 0.001$ . Sample sizes: DSS ( $n = 6$ ); BN ( $n = 8$ ). **B)** Viable conceptuses in DSS and BN strains on Day 18.5 of pregnancy. The number of viable conceptuses for the BN strain was significantly lower than that observed for the DSS strain on Day 18.5 of gestation,  $*P < 0.001$ . Sample sizes: DSS ( $n = 16$ ); BN ( $n = 16$ ). **C)** Percentage of nonviable (resorbing and/or dying) conceptuses to total (viable, resorbing and/or dying) conceptuses in DSS and BN strains on Day 18.5 of pregnancy. Nonviable conceptuses were more prevalent in the BN strain than in the DSS strain,  $*P < 0.01$ . Sample sizes: DSS ( $n = 16$ ); BN ( $n = 14$ ).

versus dead and/or resorbing conceptuses was determined. Placentation sites, including uterus, metrial gland, and placental tissues, were dissected from pregnant animals. Tissues were snap frozen in liquid nitrogen for RNA analyses. For in situ hybridization and immunocytochemistry, tissues were frozen in dry ice-cooled heptane. All tissue samples were stored at  $-80^{\circ}\text{C}$  until use. Protocols for these procedures have been described previously [12]. The University of Kansas Medical Center Animal Care and Use Committee approved all procedures for handling and experimentation with rodents.

### Immunocytochemistry and TUNEL Analyses

Immunocytochemical analyses were used to identify trophoblasts, NK cells, smooth muscle cells, and endothelial cells. Analyses were performed on 10- $\mu\text{m}$  tissue sections prepared with the aid of a cryostat and Histostain-AEC-plus kits (Zymed Laboratories, San Francisco, CA) according to the manufacturer's instructions unless stated otherwise. All immunostained tissue sections were examined and images recorded with a Leica MZFLIII stereomicroscope equipped with a CCD camera (Leica Microsystems GmbH, Welzlar, Germany).

**Trophoblast cells.** Rat invasive trophoblast cells were detected using a mouse monoclonal anti-Pan cytokeratin antibody (Sigma-Aldrich, St. Louis, MO) at a dilution of 1:400, as previously described [12].

**NK cells.** A rabbit polyclonal anti-rat perforin-1 antibody (PRF1; Torrey Pines Biolabs, Houston, TX) was used at a concentration of 2.5  $\mu\text{g}/\text{ml}$  to detect NK cells. Immunolocalization of PRF1 was visualized using alkaline phosphatase-conjugated goat anti-rabbit immunoglobulin (Sigma-Aldrich) and nitro blue tetrazolium/bromochloroindoyl phosphate (NBT/BCIP; Roche Molecular Biochemicals, Indianapolis, IN), as previously described [12].

**Endothelial cells.** Mouse monoclonal antibodies to platelet/endothelial cell adhesion molecule (PECAM; BD Pharmingen, Franklin Lakes, NJ) and to an uncharacterized rat endothelial cell-specific surface antigen (RECA1; Serotec, Oxford, UK) [13] and a rabbit polyclonal antibody to Von Willebrand Factor (VWF; Chemicon, Temecula, CA) were used to detect endothelial cells. The PECAM antibody was used at a dilution of 1:10, the RECA1 antibody at a dilution of 1:20, and the VWF antibody at a dilution of 1:100.

**Smooth muscle cells.** Smooth muscle cells were monitored with mouse monoclonal anti-smooth muscle  $\alpha$ -actin ( $\alpha$ -actin-2, ACTA2) antibodies (Sigma-Aldrich), rabbit anti-transgelin (TAGLN) antibodies (AbCam, Cambridge, MA), and mouse monoclonal antibodies to smooth muscle myosin heavy polypeptide 11 (MYH11; AbCam). The anti-ACTA2 and anti-MYH11 were used at 1:400 dilutions, and the anti-TAGLN was used at a 1:500 dilution.

**Proliferating cells.** A rabbit polyclonal antibody to MKI67 (Santa Cruz Biotechnology, Santa Cruz, CA) was used at a dilution of 1:200 to detect proliferating cells.

**TUNEL assay.** TUNEL assays were performed with In Situ Cell Death Detection Kits (Roche Applied Science, Penzberg, Germany) according to the manufacturer's instructions.

### Northern Blot Analysis

Northern blot analysis was performed as described previously [14]. Total RNA was extracted from tissues using TRIzol reagent (Invitrogen, Carlsbad, CA). Total RNA (15  $\mu\text{g}/\text{lane}$ ) was resolved in 1% formaldehyde-agarose gels, transferred to nylon membranes, and crosslinked. Blots were probed with [ $\alpha^{32}\text{P}$ ]-labeled cDNAs for prolactin-like protein-A (*Prlpa*) [15], prolactin-like protein-M (*Prlpm*) [16], and prolactin-like protein-N (*Prlpn*) [17]. Glyceraldehyde-3'-phosphate dehydrogenase (*Gapdh*) cDNA was used to evaluate the integrity and equal loading of RNA samples. At least three different tissue samples from three different animals were analyzed with each probe for each time point.

### In Situ Hybridization

In situ hybridization was performed as described previously [18]. Ten-micrometer cryosections of tissues were prepared and stored at  $-80^{\circ}\text{C}$  until use. Plasmids containing cDNAs for rat *Prlpa* [15], *Prlpm* [16], and *Prlpn* [17] were used as templates to synthesize sense and antisense digoxigenin-labeled riboprobes according to the manufacturer's instructions (Roche Molecular Biochemicals, Indianapolis, IN). Tissue sections were air dried and fixed in ice-cold 4% paraformaldehyde in phosphate-buffered saline. Prehybridizations, hybridizations, and detection of alkaline phosphatase-conjugated anti-digoxigenin were performed as previously reported [18, 19].

### Morphologic Measurements and Statistical Analysis

Morphologic measurements of intrauterine trophoblast cell invasion, thickness of the junctional zone, and uterine NK cell distributions in cross-sections of Gestation Day 18.5 placentation sites were performed with National Institutes of Health Image J software. Measurements were made from a histologic plane at the center of each placentation site perpendicular to the flat fetal surface of the placenta. Definitions of each compartment within the rat placentation site (uterine mesometrial compartment, metrial gland, mesometrial deciduum, junctional zone, and labyrinth zone) have been described [12]. The uterine mesometrial compartment is the region located between the trophoblast giant cell layer of the chorioallantoic placenta and the outer surface of the uterus. This region includes the uterine mesometrial deciduum, which is located between the trophoblast giant cell layer of the chorioallantoic placenta and the inner myometrial layer, and the metrial gland, which is situated between the inner myometrial layer and the outer surface of the uterus. The chorioallantoic placenta consists of the junctional zone and the labyrinth zone. The junctional zone comprises an area bordered by the uterine mesometrial deciduum and the labyrinth zone. It contains trophoblast giant cells, spongiotrophoblast cells, and glycogen cells. The labyrinth zone is defined as the region of the chorioallantoic placenta vascularized by the allantois. This compartment contains syncytial trophoblast, cytotrophoblast, trophoblast giant cells, and fetal mesenchyme and its associated vasculature. An estimate of intrauterine trophoblast cell invasion was determined from the ratio of cross-sectional surface area associated with the uterine mesometrial surface area infiltrated by cytokeratin-positive cells and the entire surface area of the uterine mesometrial compartment. The thickness of the junctional zone was estimated from cross-sectional area measurements of *Prlpa* mRNA-positive placental sections. Measurements were expressed as junctional zone cross-sectional area and as the ratio of junctional zone cross-sectional area to total chorioallantoic placental cross-sectional area. Uterine NK cell numbers were estimated from cross-sectional distributions of PRF1-immunopositive cells located in the uterine mesometrial compartment. A minimum of eight placentation sites from a minimum of eight different animals from each strain were examined. All statistical comparisons of mean values for DSS versus BN strains were determined by Student *t*-test. Gestational time course data on body weights and body weight gains were evaluated with analysis of variance. The source of variation from significant F-ratios was determined with Newman-Keuls multiple comparison test [20].

## RESULTS

### Pregnancy in DSS versus BN Rats

Rates of early pregnancy loss were greater in the BN strain. Approximately 40% of all BN sperm-positive females failed to possess a confirmed pregnancy on Day 18.5 of gestation (sample sizes: DSS,  $n = 19$ ; BN,  $n = 20$ ), an incidence twice that of the DSS strain. The number of viable conceptuses at Days 8.5 and 18.5 of gestation were significantly greater in DSS versus BN rats ( $P < 0.001$ ; Fig. 1, A and B).

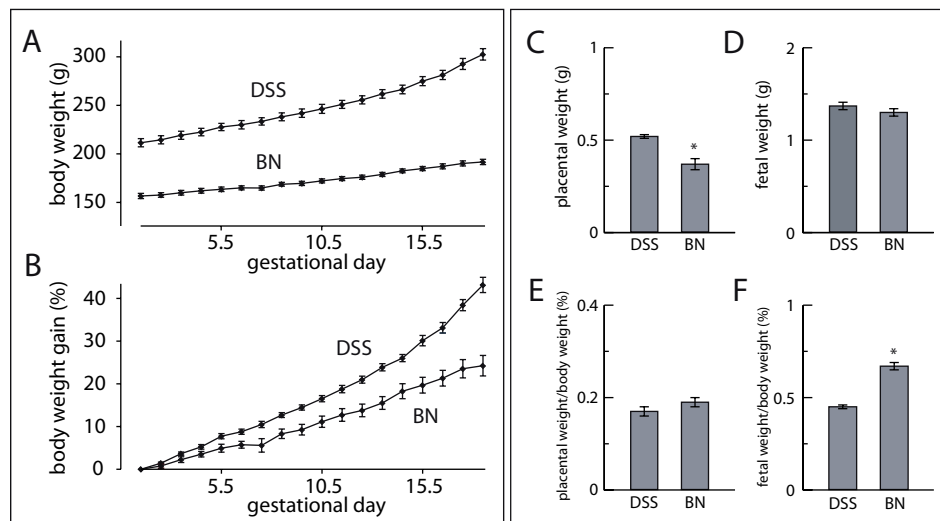


FIG. 2. Maternal, placental, and fetal responses to pregnancy in DSS and BN rat strains. **A**) Body weight (g) of the DSS and BN strains during pregnancy. DSS and BN body weights were significantly different on each day of pregnancy ( $P < 0.01$ ). **B**) Body weight gain of DSS and BN strains during pregnancy. DSS and BN body weight gain significantly diverged after Day 8.5 of pregnancy ( $P < 0.01$ ). Sample sizes for data presented in **A** and **B**: DSS ( $n = 11$ ); BN ( $n = 13$ ). **C** and **D**) Placental (**C**) and fetal (**D**) wet weights in DSS and BN strains on Day 18.5 of pregnancy. Placental weights were significantly smaller in the BN strain than in the DSS strain,  $*P < 0.001$ . **E** and **F**) Placental (**E**) and fetal (**F**) wet weights in DSS and BN strains on Day 18.5 of pregnancy expressed as a ratio to body weight. Fetal weight:body weight ratios were significantly greater for the BN strain versus the DSS strain,  $*P < 0.001$ . Sample sizes for data presented in **C–F**: DSS ( $n = 10$ ); BN ( $n = 10$ ).

Additionally, the number of resorbing and/or dying conceptuses was significantly greater at Day 18.5 of gestation in the BN strain than in the DSS strain ( $P < 0.01$ ; Fig. 1C). Collectively, the data suggest that BN rats exhibit significant problems in establishing and maintaining pregnancy.

#### Maternal, Placental, and Fetal Responses to Pregnancy

Maternal responses to pregnancy in DSS and BN rats differed, as demonstrated by body weight measurements. Female DSS rats are larger than female BN rats and gain more weight during gestation (Fig. 2, A and B).

Placental and fetal gravimetric responses to pregnancy in DSS and BN rats also were monitored on Day 18.5 of gestation (Fig. 2, C–F). Placental weights were significantly greater for the DSS strain than the BN strain ( $P < 0.001$ ; Fig. 2C). The difference is striking because there is a well-known litter size effect on placental growth [21–24], and the expectation would be larger placentas with small litters. Interestingly, there were not significant differences in fetal size. Thus, placental and

pregnancy-associated adaptations in the BN rat are sufficient to ensure fetal growth comparable to that observed in the DSS rat.

#### Genetic Differences in the Organization of the Rat Uterine Mesometrial Compartment

The organization of the maternal-fetal interface differed dramatically between the two strains. Differences were noted in the uterine mesometrial compartment and the organization of the chorioallantoic placenta. During the last week of gestation, trophoblast cells typically exit the chorioallantoic placenta and invade into the uterine mesometrial compartment, where they associate with maternal vasculature [18]. These invasive trophoblast cells can be readily distinguished from uterine stromal cells by their expression of the intermediate filament, cytokeratin, and their expression of members of the prolactin gene family. Invasion of trophoblast cells into the uterine mesometrial compartment of BN rats was significantly decreased in comparison to trophoblast invasion into the uterine mesometrial compartment of DSS rats, as detected by

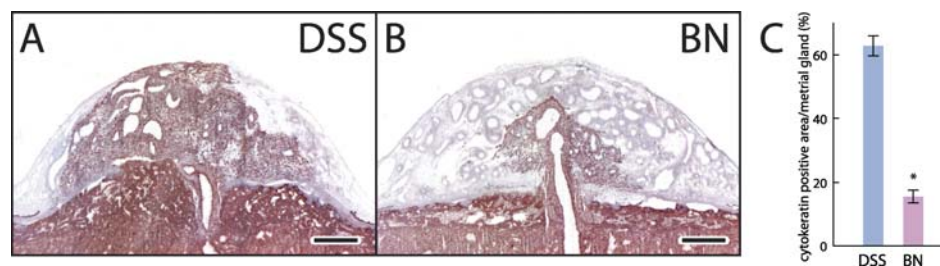
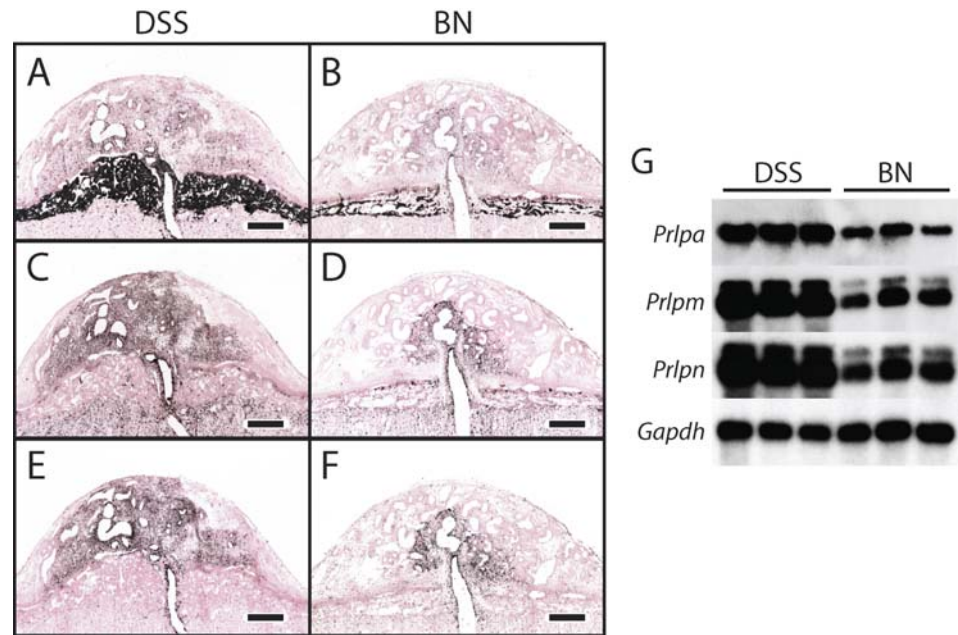


FIG. 3. Trophoblast cell invasion into the uterine mesometrial compartment. **A** and **B**) Invasive trophoblast cells were identified by cytokeratin immunostaining on tissue sections from DSS (**A**) and BN (**B**) Gestation Day 18.5 placentation sites. Chromogen: 3-amino-9-ethylcarbazole (AEC). Counterstain: hematoxylin. Bar = 1 mm. **C**) Graphic representation of ratios of cytochrome-positive cross-sectional area to total uterine mesometrial compartment cross-sectional area. Cross-sectional areas of cytochrome-positive regions and uterine mesometrial compartments were measured using National Institutes of Health Image J image analysis software. Error bars represent the standard error of the mean.  $*P < 0.001$ . Sample sizes: DSS ( $n = 8$ ); BN ( $n = 8$ ).

FIG. 4. Expression of *Prlpa*, *Prlpm*, and *Prlpn* mRNAs in the uterine mesometrial compartment. **A–F** In situ detection of mRNAs for *Prlpa* (**A** and **B**), *Prlpm* (**C** and **D**), and *Prlpn* (**E** and **F**) was performed on frozen sections from Gestation Day 18.5 placentation sites of DSS (**A**, **C**, and **E**) and BN (**B**, **D**, and **F**) strains. Sections were counterstained with nuclear fast red. Bar = 1 mm. **G** Total RNA was isolated from Gestation Day 18.5 uterine mesometrial compartments of DSS and BN strains. *Prlpa*, *Prlpm*, and *Prlpn* mRNAs were estimated by Northern blot analysis. *Gapdh* was used as a control to demonstrate integrity of the RNA and loading accuracy.



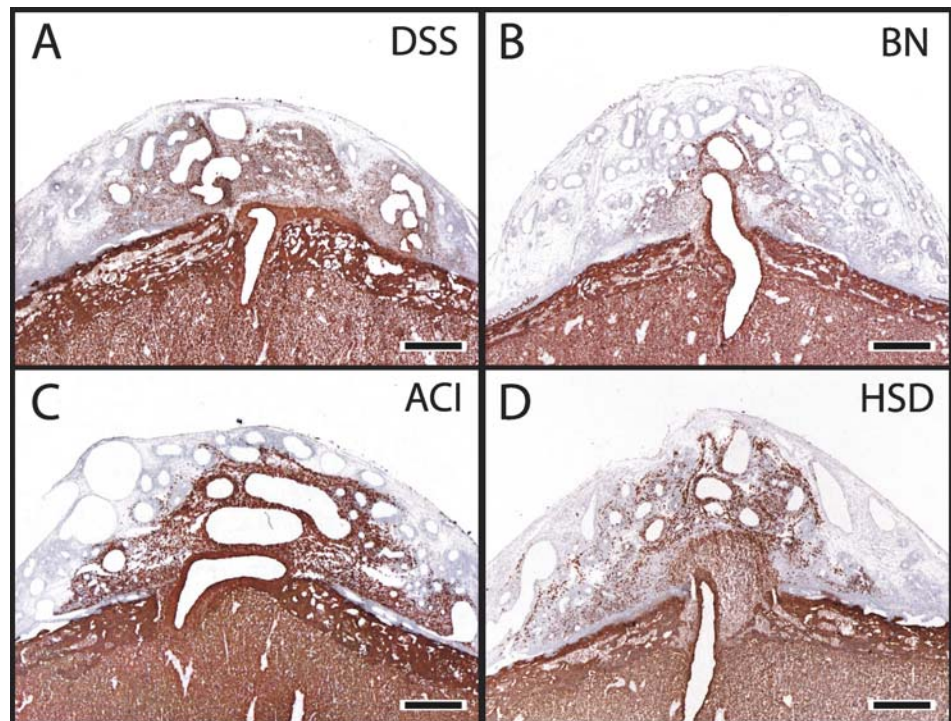
cytokeratin immunostaining ( $P < 0.001$ ) and prolactin family gene expression (*Prlpa*, *Prlpm*, and *Prlpn*; Figs. 3 and 4). DSS intrauterine trophoblast invasion was robust and comparable to intrauterine trophoblast invasion observed for the inbred ACI rat and the outbred Holtzman Sprague-Dawley rat (Fig. 5).

Invasive trophoblast cells can be distinguished based on their positioning relative to the uterine vasculature. Those cells that penetrate the vessel lumen and replace the endothelium are referred to as *endovascular invasive trophoblast cells*, and those cells that surround the vasculature are termed *interstitial invasive trophoblast cells*. Endovascular and interstitial invasive trophoblast cells could be identified within the uterine mesometrial compartments of both strains (Fig. 6). Although both types of invasive trophoblast cells are present on Day 18.5

of gestation in both strains, the overall contribution of interstitial invasive trophoblast cells was less in the BN placentation site than in the DSS site. This observation was most evident following evaluation of a gestational time course of trophoblast cell invasion (Fig. 7). On Day 15.5 of gestation, considerable interstitial trophoblast cell invasion was initiated in the DSS strain but not in the BN strain (Fig. 7, I–L).

Within the uterine mesometrial compartment of the pregnant rat there is a reciprocal relationship between invasive trophoblast cells and uterine NK cells [18]. NK cells are abundant throughout the uterine mesometrial compartment at midgestation to Gestation Day 15.5 (Fig. 8, A–L), and their distribution does not appear to differ significantly between DSS and BN rats. However, as the invasive trophoblast cells

FIG. 5. Trophoblast cell invasion into the uterine mesometrial compartment of inbred and outbred rats. Invasive trophoblast cells were identified by cytokeratin immunostaining of DSS (**A**), BN (**B**), ACI (**C**), and Holtzman Sprague-Dawley (**D**) tissues sections from Gestation Day 18.5 placentation sites. Chromogen: AEC. Counterstain: hematoxylin. Bar = 1 mm.



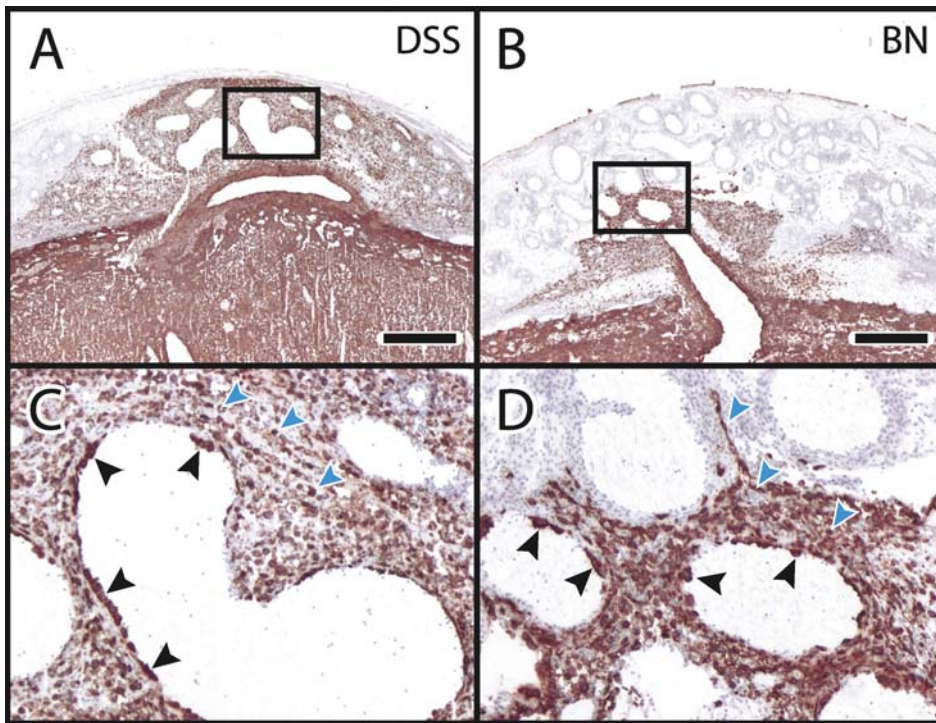


FIG. 6. Endovascular and interstitial invasion of trophoblast cells. Invasive trophoblast cells were identified by cytokeratin immunostaining of DSS (A and C) and BN (B and D) tissue sections from Gestation Day 18.5 placenta sites. C and D) Areas shown in the black outlined boxes in A and B, respectively. Black and blue arrowheads indicate endovascular and interstitial invasive trophoblast cells, respectively. Chromogen: AEC. Counterstain: hematoxylin. Bar = 1 mm.

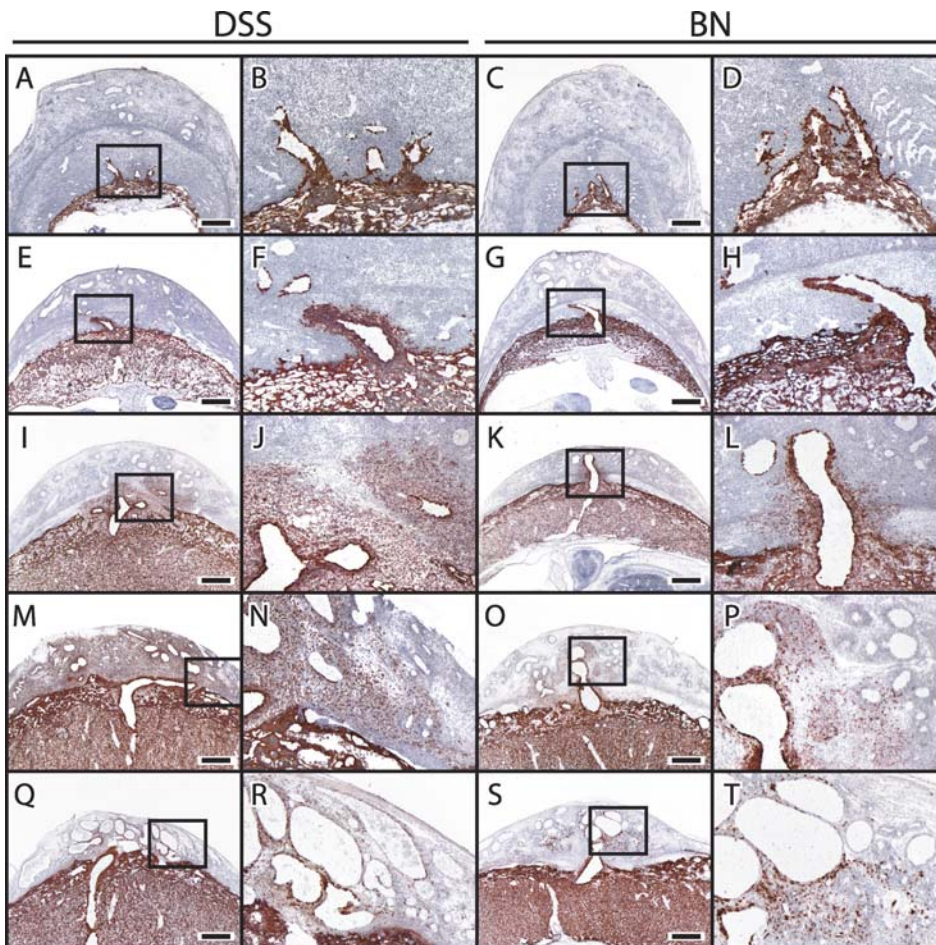
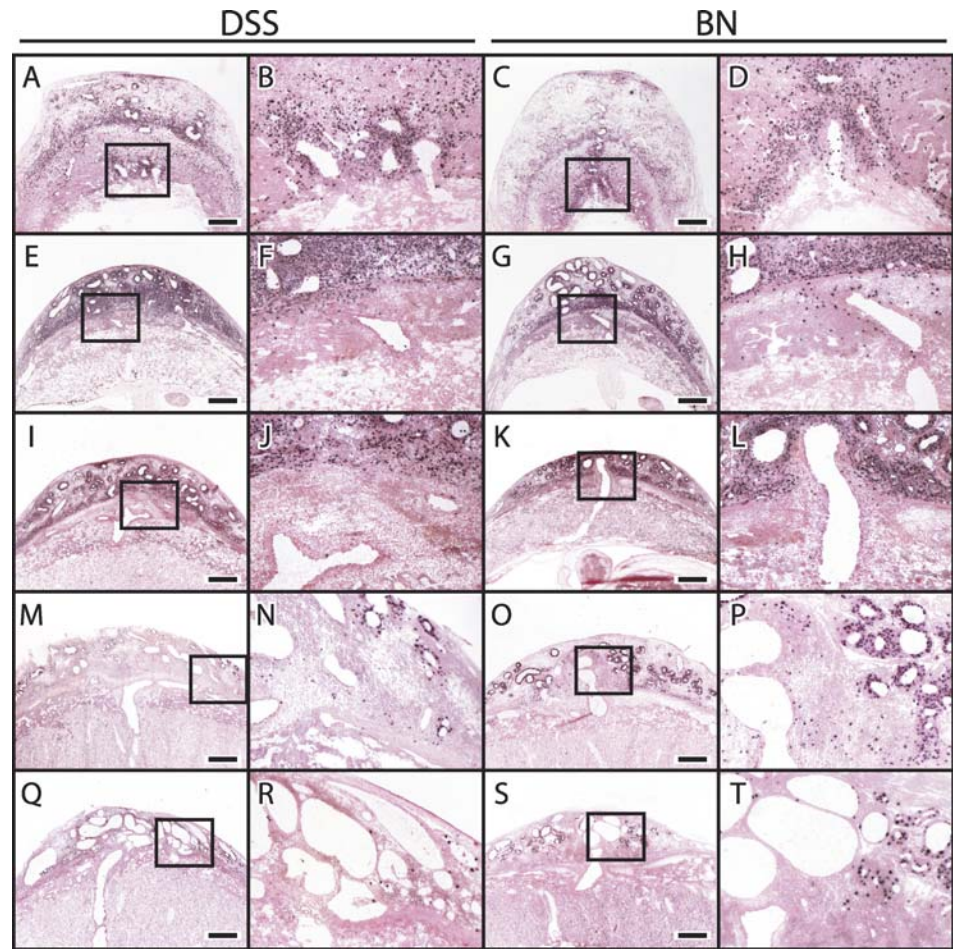


FIG. 7. Gestational time course of intra-uterine trophoblast cell invasion in DSS and BN rats. Invasive trophoblast cells were identified by cytokeratin immunostaining of DSS (first two columns of images) and BN (second two columns of images) tissue sections from Gestation Days 11.5 (A-D), 13.5 (E-H), 15.5 (I-L), 18.5 (M-P), and 21.5 (Q-T) placenta sites. Images in the second and fourth columns are high magnifications of images shown in the first and third columns (see black outlined boxes), respectively. Chromogen: AEC. Counterstain: hematoxylin. Bar = 1 mm.

FIG. 8. Gestational time course of uterine NK cell distribution in DSS and BN placentation sites. Uterine NK cells were identified by PRF1 immunostaining of DSS (first two columns of images) and BN (second two columns of images) tissue sections from Gestation Days 11.5 (A–D), 13.5 (E–H), 15.5 (I–L), 18.5 (M–P), and 21.5 (Q–T) placentation sites. Images in the second and fourth columns are high magnifications of images shown in the first and third columns (see black outlined boxes), respectively. Chromogen: NBT/BCIP. Counterstain: nuclear fast red. Bar = 1 mm.



migrate into the mesometrial compartment, NK cells disappear (Fig. 8, M–T). The reciprocal relationship is maintained in DSS and BN rat strains (Figs. 8 and 9). On Days 18.5 and 21.5 of gestation in DSS rats, uterine NK cells are few in number and are relegated to small blood vessels at the periphery of placentation sites, which represent areas devoid of invasive trophoblast cells (Figs. 8 and 9). In BN rat placentation sites, uterine NK cells are more abundant ( $P < 0.001$ ; Figs. 8 and 9). They are retained in the uterine mesometrial area lacking invasive trophoblast cells and associate with the vasculature.

Both the DSS and BN uterine mesometrial compartments are well vascularized (Fig. 10). The vascularization was demonstrated by staining with endothelial (RECA1, PECAM, and VWF) and vascular smooth muscle (ACTA2, TAGLN, MYH11) cell markers. RECA1- and VWF-immunopositive

cells (data not shown) exhibited a similar tissue distribution. However, RECA1 was easier to visualize at low magnification. Regions of the internal lining of DSS and BN uterine mesometrial vasculature were identified as possessing four different phenotypes: 1) RECA1- and PECAM-positive endothelium, 2) RECA1-positive and PECAM-negative endothelium, 3) mixed phenotype containing RECA1-positive and cytokeratin-positive cells, and 4) cytokeratin-positive trophoblast cells. Blood vessels in the central region of the uterine mesometrial compartment from both rat strains were devoid of cells expressing differentiated smooth muscle cell proteins (Fig. 11). The lack of differentiated smooth muscle cell protein expression was independent of the presence of uterine NK cells or invasive trophoblast cells.

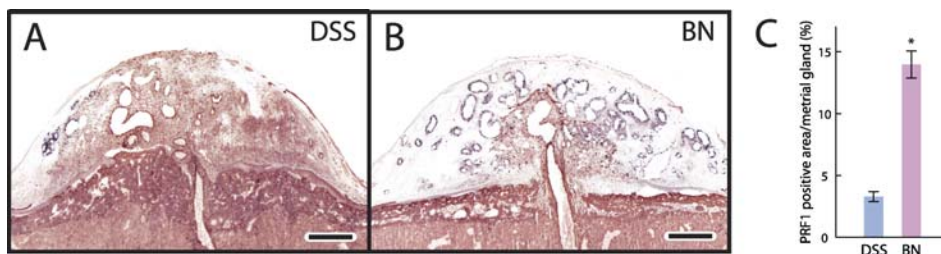


FIG. 9. Reciprocal relationship between distributions of uterine NK cells and trophoblast cells in the uterine mesometrial compartments of DSS and BN rat strains. Uterine NK cells and invasive trophoblast cells were identified by immunostaining for PRF1 and cytokeratin, respectively. Double immunostaining for PRF1 and cytokeratin was performed on frozen sections from Gestation Day 18.5 placentation sites of the DSS (A) and BN (B) strains. Chromogen: NBT/BCIP (PRF1); AEC (cytokeratin). Bar = 1 mm. C) Graphic representation of NK cell distribution in cross-sections of uterine mesometrial compartments of DSS and BN placentation sites. Error bars represent the standard error of the mean.  $*P < 0.001$ . Sample sizes: DSS ( $n = 8$ ); BN ( $n = 8$ ).

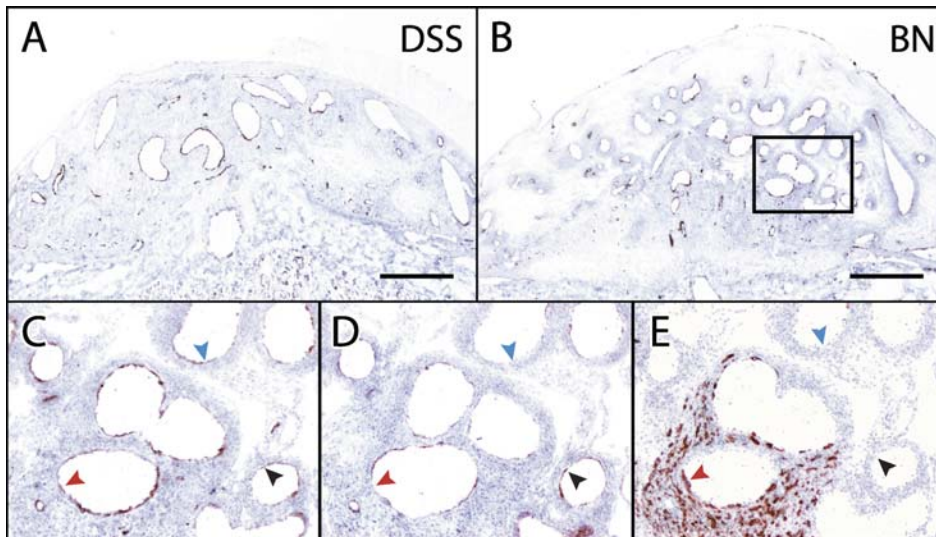


FIG. 10. Distribution of endothelial cell differentiation markers in uterine mesometrial compartments of DSS and BN rat strains. Immunostaining for RECA1 (A–C), PECAM (D), and cytokeratin (E) was performed on frozen tissue sections from Gestation Day 18.5 placentation sites of the DSS (A) and BN (B–E) rat strains. C–E) Area shown in the black outlined box in B. Chromogen: AEC. Counterstain: hematoxylin. Bar = 1 mm. Black arrowheads highlight a region of a blood vessel lined by cells staining positive for both RECA1 and PECAM but negative for cytokeratin. Red arrowheads highlight a region of a blood vessel lined by cells positive for RECA1 and cytokeratin but negative for PECAM. Blue arrowheads show a region of a blood vessel lined by cells positive for RECA1 cells but negative for PECAM and cytokeratin.

#### Genetic Differences in the Organization of the Rat Chorioallantoic Placenta

We hypothesized that strain differences in trophoblast cell invasion into the uterine mesometrial compartment could be associated with proliferation, cell death, or differentiation of the invasive trophoblast cell population. The junctional zone of the chorioallantoic placenta contains progenitors for invasive trophoblast cell differentiation [18, 25]. Proliferation (assessed by MKI67 immunostaining) and cell death (assessed by TUNEL) did not differ within the invasive trophoblast cell populations or junctional zones of DSS and BN rats (data not shown). Significant differences were noted in the sizes of the junctional zones of the two strains. The BN junctional zone was reduced in size when compared to the DSS junctional zone ( $P < 0.001$ ; Fig. 12). The genetic difference also is evident when the junctional zone area is calculated as a ratio of the entire chorioallantoic placenta. Thus, the data are consistent

with the BN rat possessing hypomorphic development of the junctional zone and its derivatives.

#### DISCUSSION

Pregnancy involves a dialogue between maternal and placental structures designed to ensure fetal development. The rat represents an intriguing model for studying the genetics of pregnancy. In this investigation we have identified quantifiable genetic traits associated with the progression of pregnancy. The DSS rat maintained on a low-salt diet exhibits a pregnancy phenotype similar to outbred Holtzman Sprague-Dawley rats [12]. The BN rat possesses a small litter size, an increased frequency of pregnancy failure, and distinct features of placentation. An overview of the strain-specific genetic differences in placentation is presented in Figure 13.

The maternal-fetal interface is a dynamic site where uterine and placental structures cooperate to promote the development of the embryo/fetus. These specialized tissues facilitate

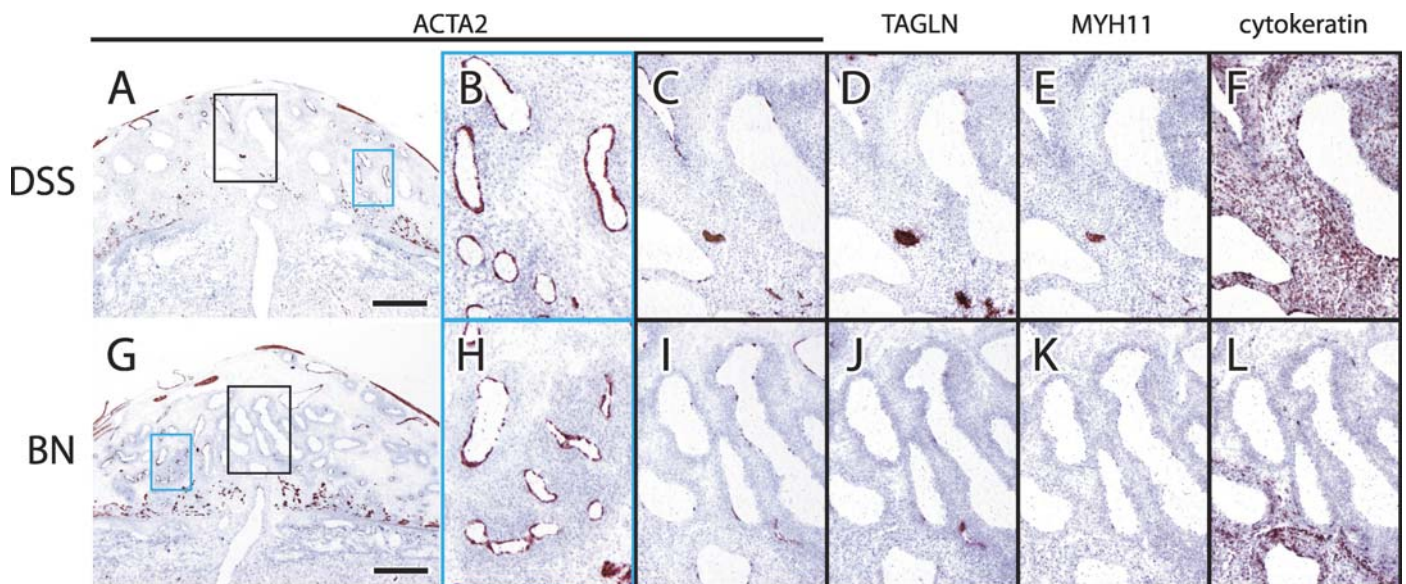


FIG. 11. Distributions of differentiated vascular smooth muscle cell proteins in the uterine mesometrial compartments of DSS and BN strains. Immunostaining for ACTA2 (A–C and G–I), TAGLN (D and J), MYH11 (E and K), and cytokeratin (F and L) were performed on serial frozen sections from Gestation Day 18.5 placentation sites of the DSS (A–F) and BN (G–L) strains. B and H) Areas shown in the blue outlined boxes present in A and G, respectively. C–F and I–L) Areas shown in the black outlined boxes present in A and G. Chromogen: AEC. Counterstain: hematoxylin. Bar = 1 mm.

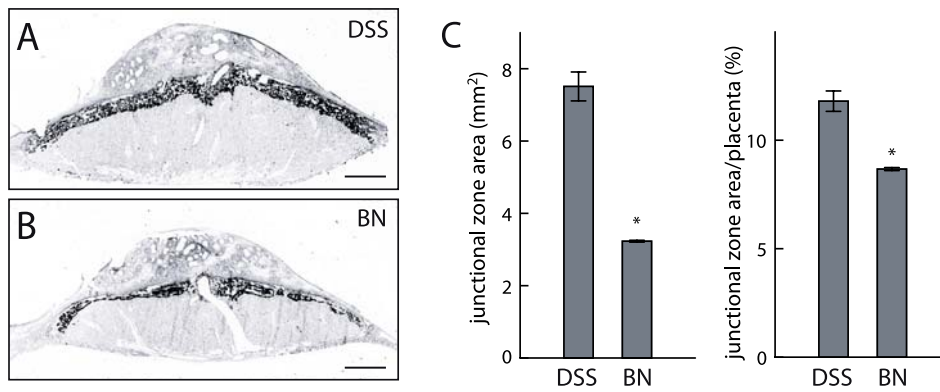


FIG. 12. Junctional zone (JZ) area in DSS and BN strains on Day 18.5 of pregnancy. **A** and **B**) In situ detection of *Prlpa* mRNA was performed on frozen sections from Gestation Day 18.5 placental sites of DSS (**A**) and BN (**B**) strains. Sections were counterstained with nuclear fast red. Bar = 2 mm. **C**) Graphic representations of the cross-sectional area of the junctional zone. Cross-sectional areas of junctional zones of Gestation Day 18.5 placental sites were measured using National Institutes of Health Image J image analysis software. Junctional zone was determined based on *Prlpa* mRNA-positive placental sections from Gestation Day 18.5 placental sites of DSS and BN strains. Error bars represent the standard error of the mean. \* $P < 0.001$ . Sample sizes: DSS (n = 8); BN (n = 8).

efficient nutrient delivery. The rat possesses a hemochorial placenta [25, 26]. This type of placentation is characterized by erosion of the maternal uterine epithelium and vasculature, permitting the direct flow of maternal nutrients to trophoblast cells. Cellular specializations develop that facilitate trophoblast cell interactions with two vascular beds. Trophoblast cells connected to the maternal vasculature specialize in facilitating nutrient flow to the placenta, whereas trophoblast cells developing in proximity to the fetal vasculature promote nutrient transfer to the fetus. DSS and BN rat strains represent extremes in the extent of intrauterine trophoblast cell invasion. DSS intrauterine trophoblast cell invasion is robust, whereas BN intrauterine trophoblast cell invasion is modest in comparison. The inference is that the DSS invasive trophoblast cell trait, which is similar to that of outbred rats and at least two other inbred strains (ACI, Fischer F344) [present study, 18, 27], may favor efficient delivery of nutrients from the maternal vasculature to the placenta. Invasive trophoblast cells associate with uterine spiral arteries supplying the mesometrial uterine compartment, and the uterine spiral arteries undergo a pregnancy-specific modification [18, 28–30]. Invasive trophoblast cells are likely involved in this vascular remodeling; however, the specific tasks they perform are not well understood.

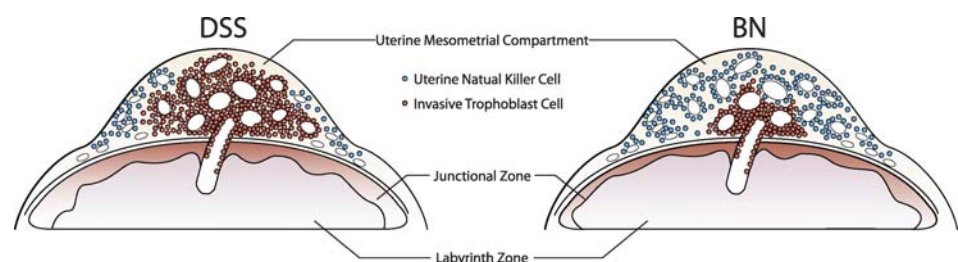
Invasive trophoblast cells consist of two apparently distinct lineages: endovascular and interstitial [18, 27–30]. Endovascular trophoblast cells replace the endothelium of the uterine mesometrial spiral arteries, whereas interstitial trophoblast cells surround these uterine vessels. Phenotypic differences in endovascular versus interstitial invasive trophoblast cells were reported previously [27]. Although both invasive trophoblast cell lineages are present in DSS and BN rats, the size of the interstitial invasive trophoblast cell population was notably smaller in the BN placentation site, especially when observed

at Gestation Day 15.5. These observations suggest that at least some aspects of the regulation of the two invasive trophoblast cell lineages are independently controlled.

Factors underlying differences in DSS and BN rat trophoblast cell invasion were not initially apparent. In the current study, invasive trophoblast cells of the two rat strains did not appear to differ in their proliferative capacity (MKI67 staining) or their apoptotic index (TUNEL staining). A prominent difference was observed in the junctional zones of the two strains. The BN junctional zone is significantly smaller than the DSS junctional zone. Since the junctional zone is the source of invasive trophoblast cell progenitors [18, 25], it is plausible that the limited BN trophoblast cell invasion was related to the growth-restricted BN junctional zone. A number of genes have been identified as critical to junctional zone development through mouse gene targeting experiments. These genes include: Cbp/p300-interacting transactivator with Glu/Asp-rich carboxy-terminal domain, 2 (*Cited2*) [31], epidermal growth factor receptor (*Egfr*) [32, 33], achaete-scute complex homolog-like 2 (*Ascl2*) [34–36], pleckstrin homology-like domain, family A, member 2 (*Phlda2*) [37, 38], B-Raf (*Braf*) [39], keratins 8 and 19 [40], cullin 7 (*Cul7*) [41], heat shock factor 1 (*HSF1*) [42], nuclear receptor coactivator 6 (*Ncoa6*) [43], gap junction membrane channel protein  $\beta$ 3 (*Gjb3*) [44], chorioredermia (*Chm*) [45], and those associated with hypoxia-inducible factor signaling [46–48]. In addition, nutrient availability is a known regulator of junctional zone development [49, 50]. Whether any of the junctional zone development regulatory genes are dysregulated or dysfunctional in the BN rat remain to be determined.

BN rat placentation is associated with apparent adaptive responses in the uterine mesometrial compartment. The compensatory reactions include the persistence of mesometrial uterine NK cells into late gestation. Uterine NK cells are

FIG. 13. Schematic representations of placentation sites for DSS (left panel) and BN (right panel) rat strains on Day 18.5 of gestation. The schematic diagram illustrates invasive trophoblast cell populations, uterine NK cell distributions, uterine mesometrial vasculature, and chorioallantoic placental organization in the two rat strains.



prominent at midgestation in the rat [18, 51] and mouse [52, 53] and during early pregnancy in the human [54]. At least in part, they are viewed as modulators of the uterine vasculature [55, 56]. As gestation progresses they disappear and are functionally replaced, to some extent, by invasive trophoblast cells [18]. Although the regulation of uterine NK cell trafficking and demise is not well understood, uterine NK cells do exhibit a reciprocal relationship with intrauterine invasive trophoblast cells [18]. Some speculations can be offered regarding the relationship between uterine NK cells and invasive trophoblast cells. First of all, limited trophoblast cell invasion in the BN rat may be the result of the overabundance of uterine NK cells. Such a hypothesis is consistent with previous results indicating that uterine NK cells and their products can inhibit intrauterine trophoblast cell invasion [18, 57, 58]. However, such observations are not consistent with a recent report suggesting that uterine NK cells may actually promote trophoblast invasion [59]. There also is some evidence that BN rat NK cells are phenotypically distinct [60], which may contribute to their unusual composition and possibly actions in the BN uterine mesometrial compartment. Finally, as indicated above, the BN placentation phenotype may be intrinsic to BN trophoblast cells. Uterine NK cells and invasive trophoblast cells may be viewed as two complementary mediators of uterine mesometrial vascular remodeling. During midgestation, uterine NK cells initiate vascular remodeling, and then as gestation progresses are replaced by invasive trophoblast cells. If the development of invasive trophoblast cells is limited, as in the BN rat, then uterine NK cells persist, representing the predominant effector of the uterine vasculature. Although BN placentation differs from placentation in other rat strains, it can be effective, as demonstrated by monitoring fetal weight. Thus, maternal adaptations, such as those associated with the uterine NK cells, may be particularly important for the success of the BN pregnancy.

The quantifiable trait differences in placentation can be exploited to discover regulatory genes controlling placentation. The genetic control of physiologic processes can be investigated with chromosome-substituted inbred strains of rats. Chromosome-substituted rat strains have been generated with BN chromosomes introgressed into the DSS inbred strain [61]. The BN rat genome also represents the genome sequenced for the rat genome project [62]. Analyses of chromosome-substituted strains of mice and rats have proved to be effective tools for ascribing function to the genome [61, 63, 64]. DSS-BN chromosome-substituted strains should provide a tool for the discovery of genes critical to pregnancy regulation and placentation.

In conclusion, the data indicate that BN rats exhibit a unique pattern of placentation and may represent an excellent model for investigating the genetics of placental development.

## ACKNOWLEDGMENTS

We would like to thank Dr. Allen Cowley of Medical College of Wisconsin and his staff for insights and information about working with the BN and DSS rat strains.

## REFERENCES

- Ralston A, Rossant J. Genetic regulation of stem cell origins in the mouse embryo. *Clin Genet* 2005; 68:106–112.
- Wang H, Dey SK. Roadmap to embryo implantation: clues from mouse models. *Nat Rev Genet* 2006; 7:185–199.
- Sargent IL. Maternal and fetal immune responses during pregnancy. *Exp Clin Immunogenet* 1993; 10:85–102.
- Sibai BM, Frangieh A. Maternal adaptation to pregnancy. *Curr Opin Obstet Gynecol* 1995; 7:420–426.
- Granger JP. Maternal and fetal adaptations during pregnancy: lessons in regulatory and integrative physiology. *Am J Physiol Regul Integr Comp Physiol* 2002; 283:R1289–R1292.
- Bateson P, Barker D, Clutton-Brock T, Deb D, D'Udine B, Foley RA, Gluckman P, Godfrey K, Kirkwood T, Lahr MM, McNamara J, Metcalfe NB, et al. Developmental plasticity and human health. *Nature* 2004; 430:419–421.
- Gluckman PD, Hanson MA. Living with the past: evolution, development, and patterns of disease. *Science* 2004; 305:1733–1736.
- Nathanielsz PW. Animal models that elucidate basic principles of the developmental origins of adult diseases. *ILAR J* 2006; 47:73–82.
- Cowley AW. Genomics and homeostasis. *Am J Physiol* 2003; 284:R611–R627.
- Gill TJ 3rd, Kunz HW, Hansen CT. Litter sizes in inbred strains of rats (*Rattus norvegicus*). *J Immunogenet* 1979; 6:461–463.
- Dene H, Rapp JP. Maternal effects on blood pressure and survivability in inbred Dahl salt-sensitive rats. *Hypertension* 1985; 7:767–774.
- Ain R, Konno T, Canham LN, Soares MJ. Phenotypic analysis of the placenta in the rat. In: Soares MJ, Hunt JS (eds.), *Placenta and Trophoblast: Methods and Protocols*, vol. 1. Totowa, NJ: Humana Press; 2006:295–313.
- Duijvestijn AM, van Goor H, Klatter F, Majoor GD, van Bussel E, van Breda Vriesman PJ. Antibodies defining rat endothelial cells: RECA-1, a pan-endothelial cell-specific monoclonal antibody. *Lab Invest* 1992; 66:459–466.
- Faria TN, Deb S, Kwok SCM, Talamantes F, Soares MJ. Ontogeny of placental lactogen-I and placental lactogen-II expression in the developing rat placenta. *Dev Biol* 1990; 141:279–291.
- Duckworth ML, Peden LM, Friesen HG. Isolation of a novel prolactin-like cDNA clone from developing rat placenta. *J Biol Chem* 1986; 61:10879–10884.
- Dai G, Lu L, Tang S, Peal MJ, Soares MJ. The prolactin family miniarray: a tool for evaluating uteroplacental/trophoblast endocrine phenotypes. *Reproduction* 2002; 124:755–765.
- Wiemers DO, Ain R, Ohboshi S, Soares MJ. Migratory trophoblast cells express a newly identified member of the prolactin gene family. *J Endocrinol* 2003; 179:335–346.
- Ain R, Canham LN, Soares MJ. Gestation stage-dependent intrauterine trophoblast cell invasion in the rat and mouse: novel endocrine phenotype and regulation. *Dev Biol* 2003; 260:176–190.
- Wiemers DO, Shao LJ, Ain R, Dai G, Soares MJ. The mouse prolactin family locus. *Endocrinology* 2003; 144:313–325.
- Keppel G. *Design and Analysis*. Englewood Cliffs, NJ: Prentice Hall; 1973.
- McLaren A. Genetic and environmental effects of foetal and placental growth in mice. *J Reprod Fertil* 1965; 9:79–98.
- Croskerry PG, Smith GK, Hall S, Shepard BJ. Fetal and placental growth in the rat following differential reduction of litter size. *Biol Neonate* 1978; 33:31–38.
- Norman NA, Bruce NW. Fetal and placental weight relationships in the rat at days 13 and 17 of gestation. *J Reprod Fertil* 1979; 57:345–348.
- Norman NA, Bruce NW. Fetal and placental weight relationships in the albino rat near term. *Teratology* 1979; 19:245–250.
- Davies J, Glasser SR. Histological and fine structural observations on the placenta of the rat. *Acta Anat* 1968; 69:542–608.
- Enders AC, Welsh AO. Structural interactions of trophoblast and uterus during hemochorial placenta formation. *J Exp Zool* 1993; 266:578–587.
- Arroyo JA, Konno T, Khalili DC, Soares MJ. A simple in vivo approach to investigate invasive trophoblast cells. *Int J Dev Biol* 2005; 49:977–980.
- Caluwaerts S, Vercruyse L, Luyten C, Pijnenborg R. Endovascular trophoblast invasion and associated structural changes in uterine spiral arteries of the pregnant rat. *Placenta* 2005; 26:574–584.
- Pijnenborg R, Vercruyse L, Hanssens M. The uterine spiral arteries in human pregnancy: facts and controversies. *Placenta* 2006; 27:939–958.
- Vercruyse L, Caluwaerts S, Luyten C, Pijnenborg R. Interstitial trophoblast invasion in the decidua and mesometrial triangle during the last third of pregnancy in the rat. *Placenta* 2006; 27:22–33.
- Withington SL, Scott AN, Saunders DN, Floro KL, Preis JI, Michalick J, Maclean K, Sparrow DB, Martinez Barbera JP, Dunwoodie SL. Loss of *Cited2* affects trophoblast formation and vascularization of the placenta. *Dev Biol* 2006; 294:67–82.
- Sibilia M, Wagner EF. Strain-dependent epithelial defects in mice lacking the EGF receptor. *Science* 1995; 269:234–238.
- Threadgill DW, Dlugosz AA, Hansen LA, Tennenbaum T, Lichti U, Yee D, LaMantia C, Mourton T, Herrup K, Harris RC, Barnard JA, Yuspa SH, Coffey RJ, Magnuson T. Targeted disruption of mouse EGF receptor:

- effect of genetic background on mutant phenotype. *Science* 1995; 269: 230–234.
34. Guillemot F, Caspary T, Tilghman SM, Copeland NG, Gilbert DJ, Jenkins NA, Anderson DJ, Joyner AL, Rossant J, Nagy A. Genomic imprinting of *Mash2*, a mouse gene required for trophoblast development. *Nat Genet* 1995; 9:235–242.
  35. Guillemot F, Nagy A, Auerbach A, Rossant J, Joyner AL. Essential role of *Mash-2* in extraembryonic development. *Nature* 1994; 371:333–336.
  36. Tanaka M, Gertsenstein M, Rossant J, Nagy A. *Mash2* acts cell autonomously in mouse spongiotrophoblast development. *Dev Biol* 1997 190: 55–65.
  37. Frank D, Fortino W, Clark L, Musalo R, Wang W, Saxena A, Li CM, Reik W, Ludwig T, Tycko B. Placental overgrowth in mice lacking the imprinted gene *Ipl*. *Proc Natl Acad Sci U S A* 2002; 99:7490–7495.
  38. Salas M, John R, Saxena A, Barton S, Frank D, Fitzpatrick G, Higgins MJ, Tycko B. Placental growth retardation due to loss of imprinting of *Phlda2*. *Mech Dev* 2004; 121:1199–1210.
  39. Galbanova-Kovacs G, Matzen D, Piazzolla D, Meissi K, Plyushch T, Chen AP, Silva A, Baccarini M. Essential role of B-Raf in Erk activation during extraembryonic development. *Proc Natl Acad Sci U S A* 2006; 103:1325–1330.
  40. Tamai Y, Ishikawa T, Bosl MR, Mori M, Nozaki M, Baribault H, Oshima RG, Taketo MM. Cytokeratins 8 and 19 in the mouse placental development. *J Cell Biol* 2000; 151:563–572.
  41. Arai T, Kasper JS, Skaar JR, Ali SH, Takahashi C, DeCaprio JA. Targeted disruption of *p185/Cul7* gene results in abnormal vascular morphogenesis. *Proc Natl Acad Sci U S A* 2003; 100:9855–9860.
  42. Xiao X, Zuo X, Davis AA, McMillian DR, Curry BB, Richardson JA, Benjamin IJ. HSF1 is required for extra-embryonic development, postnatal growth and protection during inflammatory responses in mice. *EMBO J* 1999; 18:5943–5952.
  43. Antonson P, Schuster GU, Wang L, Rozell B, Holter E, Flodby P, Treuter E, Holmgren L, Gustafsson JA. Inactivation of the nuclear receptor coactivators *RAP250* in mice in placental vascular dysfunction. *Mol Cell Biol* 2003; 23:1260–1268.
  44. Plum A, Winterhager E, Pesch J, Lautermann J, Hallas G, Rosentreter B, Traub O, Herberhold C, Willecke K. *Connexin31*-deficiency in mice causes transient placental dysmorphogenesis but does not impair hearing and skin differentiation. *Dev Biol* 2001; 231:334–347.
  45. Shi W, van den Hurk JAJM, Alamo-Bethencourt V, Mayer W, Winkens HJ, Ropers HH, Cremers FPM, Fundele R. *Chorioderemia* gene product affects trophoblast development and vascularization in mouse extra-embryonic tissues. *Dev Biol* 2004; 272:53–65.
  46. Adelman DM, Gertsenstein M, Nagy A, Simon MC, Maltepe E. Placental cell fates are regulated in vivo by HIF-mediated hypoxia responses. *Genes Dev* 2000; 14:3191–3203.
  47. Cowden Dahl KD, Fryer BH, Mack FA, Compennolle V, Maltepe E, Adelman DM, Carmeliet P, Simon MC. Hypoxia-inducible factors  $1\alpha$  and  $2\alpha$  regulate trophoblast differentiation. *Mol Cell Biol* 2005; 25:10479–10491.
  48. Maltepe E, Krampitz GW, Okazaki KM, Red-Horse K, Mak W, Simon MC, Fisher SJ. Hypoxia-inducible factor-dependent histone deacetylase activity determines stem cell fate in the placenta. *Development* 2005; 132: 3393–3403.
  49. Doherty CB, Lewis RM, Sharkey A, Burton GJ. Placental composition and surface area but not vascularization are altered by maternal protein restriction in the rat. *Placenta* 2003; 24:34–38.
  50. Fryer BH, Simon MC. Hypoxia, HIF and the placenta. *Cell Cycle* 2006; 5: 495–498.
  51. Head JR. Uterine natural killer cells during pregnancy in rodents. *Nat Immun* 1996; 15:7–21.
  52. Croy BA, Luross JA, Guimond MJ, Hunt JS. Uterine natural killer cells: insights into lineage relationships and functions from studies of pregnancies in mutant and transgenic mice. *Nat Immun* 1996; 15:22–33.
  53. Liu CC, Young JDE. Uterine natural killer cells in the pregnant uterus. *Adv Immunol* 2001; 79:297–329.
  54. Bulmer JN, Lash GE. Human uterine natural killer cells: a reappraisal. *Mol Immunol* 2005; 42:511–521.
  55. Croy BA, Ashkar AA, Minhas K, Greenwood JD. Can murine uterine natural killer cells give insights into the pathogenesis of pre-eclampsia? *J Soc Gynecol Invest* 2000; 7:12–20.
  56. Croy BA, Chantakru S, Esadeg S, Ashkar AA, Wei Q. Decidual natural killer cells: key regulators of placental development. *J Reprod Immunol* 2002; 57:151–168.
  57. Hu Y, Dutz JP, MacCalman CD, Yong P, Tan R, von Dadelszen P. Decidual NK cells alter in vitro first trimester cytotrophoblast migration: a role for IFN- $\gamma$ . *J Immunol* 2006; 177:8522–8530.
  58. Lash GE, Otun HA, Innes BA, Kirkley M, De Oliveira L, Searle RF, Robson SC, Bulmer JN. Interferon- $\gamma$  inhibits extravillous trophoblast cell invasion by a mechanism that involves both changes in apoptosis and protease levels. *FASEB J* 2006;25:12–2518.
  59. Hanna J, Goldman-Wohl D, Hamani Y, Avraham I, Greenfield C, Natanson-Yaron S, Prus D, Cohen-Daniel L, Amon TI, Manaster I, Gazit R, Yutkin V, et al. Decidual NK cells regulate key developmental processes at the human fetal-maternal interface. *Nat Med* 2006; 12:1065–1074.
  60. Mikus LD, Rosenthal LA, Sorkness RL, Lemanske RF Jr. Reduced interferon-gamma secretion by natural killer cells from rats susceptible to postviral chronic airway dysfunction. *Am J Respir Cell Mol Biol* 2001; 24: 74–82.
  61. Cowley AW, Roman RJ, Jacob HJ. Application of chromosomal substitution techniques in gene-function discovery. *J Physiol* 2004; 554: 46–55.
  62. Rat Genome Sequencing Project Consortium. Genome sequence of the Brown Norway rat yields insights into mammalian evolution. *Nature* 2004; 428:493–521.
  63. Nadeau JH, Singer JB, Matin A, Lander ES. Analysing complex genetic traits with chromosome substitution strains. *Nat Genet* 2000; 24:221–225.
  64. Singer J, Hill AE, Burrage LC, Olszens KR, Song J, Justice M, O'Brien WE, Conti DV, Witte JS, Lander ES, Nadeau JH. Genetic dissection of complex traits with chromosome substitution strains of mice. *Science* 2004; 304:445–448.